Hot surface ignition dynamics in hydrogen-air mixtures near the flammability limits

L. R. Boeck, J. Melguizo-Gavilanes and J. E. Shepherd
Graduate Aerospace Laboratories, California Institute of Technology
Pasadena, CA, USA

1 Introduction

Ignition of premixed hydrogen-air from a hot surface in a closed vessel is considered with a particular focus on explosion dynamics near the flammability limits. The terms flammability limit and explosion limit describe two different limits of interest: the former evaluates the general possibility to establish a self-sustained flame in a given mixture, whereas the latter delineates explosions with negligible and strong pressure increase. For premixed hydrogen-air, the lower and upper flammability limits are $X_{\mathrm{H_2}} = 4.0\%$ and $X_{\mathrm{H_2}} = 75.0\%$, respectively. The lower explosion limit (8%) differs from the lower flammability limit, whereas the upper limits coincide. Between the lower flammability limit and the lower explosion limit, cyclic flame propagation has been observed [1]. The present work extends this study using a combined experimental and numerical approach.

2 Experimental setup

Ignition experiments were conducted in a $2.2\,\mathrm{L}$ vessel with internal dimensions $0.114\,\mathrm{m} \times 0.114\,\mathrm{m} \times 0.165\,\mathrm{m}$. The hot surface, a cylindrical Autolite 1110 glow plug with a stainless steel 316 surface, was mounted vertically in the lower section of the vessel and equipped with a stagnation plate [1, 2]. The glow plug diameter was $5.1\,\mathrm{mm}$, the height above the stagnation plate exposed to the mixture was $9.3\,\mathrm{mm}$. The vessel was filled with hydrogen, oxygen and nitrogen ($X_{\mathrm{O_2}} : X_{\mathrm{N_2}} = 1 : 3.76$) using the method of partial pressures with a $10\,\mathrm{Pa}$ accuracy. The components were mixed by a circulation pump and left to settle. The initial conditions were $P_o = 101.3\,\mathrm{kPa}$ and $T_o = 295\,\mathrm{K}$. Supplying electrical current to the glow plug started the heating process. Each experiment was terminated after $60\,\mathrm{s}$.

Ignition was characterized in terms of surface temperature and flame propagation dynamics. The surface temperature was measured by two-color pyrometry. The pyrometer setup and its calibration using a blackbody radiation source was described in [3] along with the definition of measurement uncertainty. Ignition dynamics were captured by Mach-Zehnder interferometry using a Phantom V7-11 high speed camera. The optical phase difference $\Delta\varphi$ between rays of light at wavelength λ passing through the test section along the z-axis (perpendicular the the x-y plane shown in following figures) between coordinates ξ_1 and ξ_2 and the reference path of the interferometer writes

$$\Delta\varphi = \frac{2\pi}{\lambda} \int_{\xi_1}^{\xi_2} [n(z) - n_0]\,\mathrm{d}z. \tag{1}$$

Correspondence to: lorenz.boeck@fmglobal.com

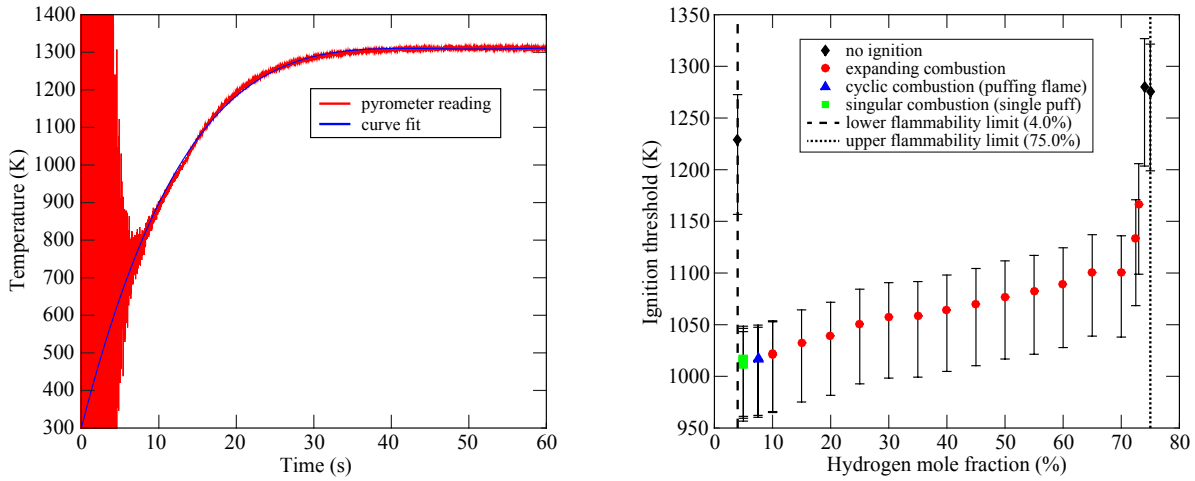

Figure 1: Left: glow plug heating measured by pyrometry (red) and approximated by a polynomial (blue). Right: ignition threshold and ignition regimes (markers) as a function of hydrogen mole fraction.

In Eq. 1, $n(z)$ is the gas refractive index in the test section and n_0 is the refractive index at initial conditions. The optical phase difference was obtained from interferograms by 2-D Windowed Fourier Transformation [4]. Since the flow field was symmetric about the glow plug axis, Abel inversion [5] could be applied to determine the refractive index in the center plane of the glow plug. The Lorenz-Lorentz equation related the refractive index to the gas density ρ, $R_L = (n^2-1)/(n^2+2)\cdot W/\rho$, where R_L and W are the molar refractivity and molar mass of the mixture, respectively. Molar refractivities were taken from [6]. The ideal gas law yielded the gas temperature.

3 Computational methodology

The motion, transport and chemical reaction in the gas surrounding the glow plug were modeled using the low Mach number, variable-density reactive Navier-Stokes equations with temperature-dependent transport properties [7]. Differential diffusion effects were taken into account using a constant but non-unity Lewis number for each species as proposed by [7]. A detailed description of the model can be found in [8]. The governing equations were solved in an axisymmetric 2-D geometry using the OpenFOAM toolbox [9]. The chemistry was modeled using Mével's mechanism for hydrogen oxidation which includes 9 species and 21 reactions [10, 11].

The computational domain was discretized with 200,000 cells, compressed near the wall of the glow plug with a minimum cell size of $80\,\mu$m, to resolve the thermal and hydrodynamic boundary layers. The initial conditions were $P_o = 101\,$kPa, $T_o = 300\,$K, $U_o = (0,0,0)\,$m/s, and mass fractions $Y_{\mathrm{H_2}}$ = 0.00364, $Y_{\mathrm{O_2}}$ = 0.23216, $Y_{\mathrm{N_2}}$ = 0.7642, corresponding to a hydrogen mole fraction of $X_{\mathrm{H_2}}$ = 5%. No-slip boundary condition and constant temperature $T_{wall} = T_o$ were imposed on the vessel walls. On the glow plug surface, the experimental heating ramp measured by pyrometry shown in Fig. 1 (left, curve fit) was imposed. The full problem was integrated, allowing it to naturally ignite and flame propagation to occur, without artificially igniting the mixture or imposing a prescribed flame speed as was done in [1].

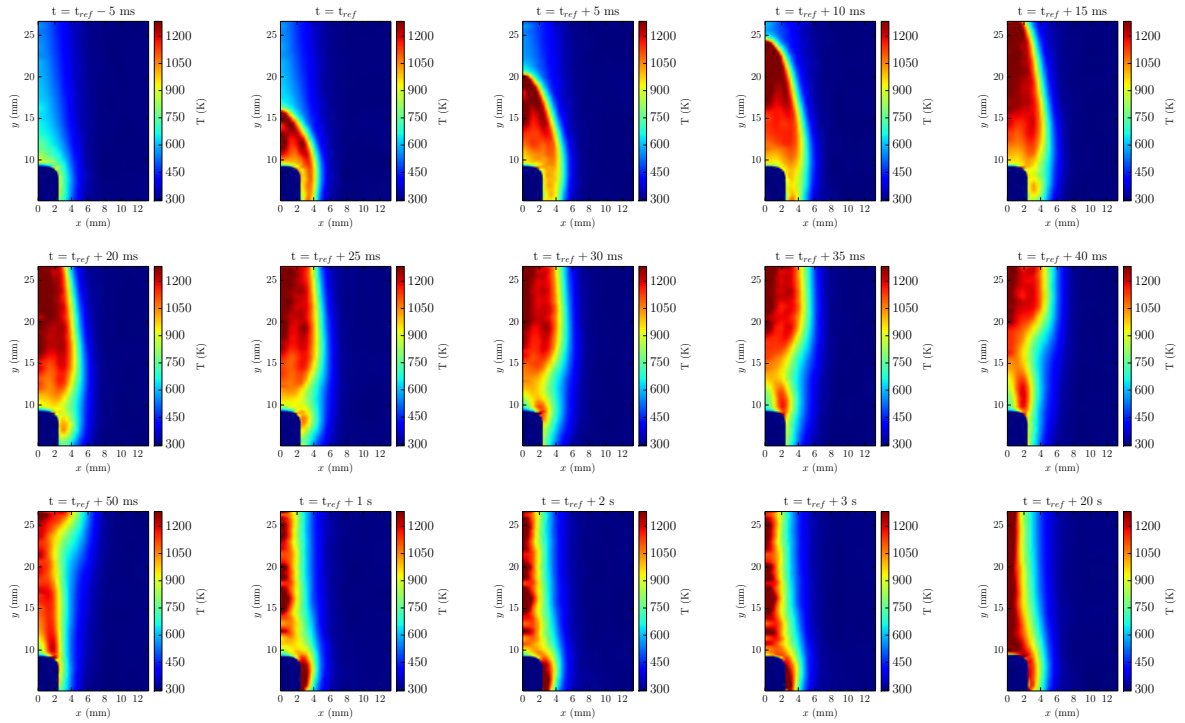

Figure 2: Single puff ignition in 5% hydrogen/air mixture, temperature fields from interferometry.

4 Experimental results

4.1 Glow plug heating and ignition temperatures

The glow plug current and voltage were chosen such that fast initial heating was achieved and temperature was stabilized subsequently, see Fig. 1 (left). Figure 1 (right) presents ignition thresholds, corresponding to the surface temperature at the time of ignition. The following ignition regimes were observed: (i) At $X_{\mathrm{H_2}} \geq 10\%$, expanding flames occurred with a steady consumption of the entire vessel volume; (ii) At $X_{\mathrm{H_2}} = 7.5\%$, cyclic (puffing) combustion took place. Cyclic combustion occurs due to the competition of combustion-induced flow and the flame in mixtures with low flame speeds. After ignition, the flame travels upward along the thermal plume rapidly and induces flow at its base, which locally exceeds the flame propagation speed and gives rise to repeated puffing [1, 2]; (iii) At $X_{\mathrm{H_2}} = 5\%$, we observed singular ignition events (single puff) which have been mentioned, but not examined in detail by Boettcher [2]. The nature of this regime is discussed in the following. Note that neither cyclic combustion nor single puff ignition was observed near the upper flammability limit.

4.2 Dynamics of single-puff ignition

Temperature fields from interferometry are presented in Fig. 2 for $X_{\mathrm{H_2}} = 5\%$. Time is given for each frame taking the observed time of ignition as a reference. The first frame, $t = t_{ref} - 5\,\mathrm{ms}$, corresponds to a glow plug surface temperature of 1010 K, shortly before ignition. Between this frame and $t = t_{ref}$ an ignition kernel forms at the top of the glow plug. The flame is subsequently advected upward inside the thermal plume. It reaches a maximum radius of about 5 mm at $t = t_{ref} + 15\,\mathrm{ms}$. At $t = t_{ref} + 30\,\mathrm{ms}$, a flame perturbation (concave flame section) appears at $y \approx 12.5\,\mathrm{mm}$ and $2\,\mathrm{mm} \leq x \leq 5\,\mathrm{mm}$ which grows over time and propagates upwards. A localized hot region indicating chemical

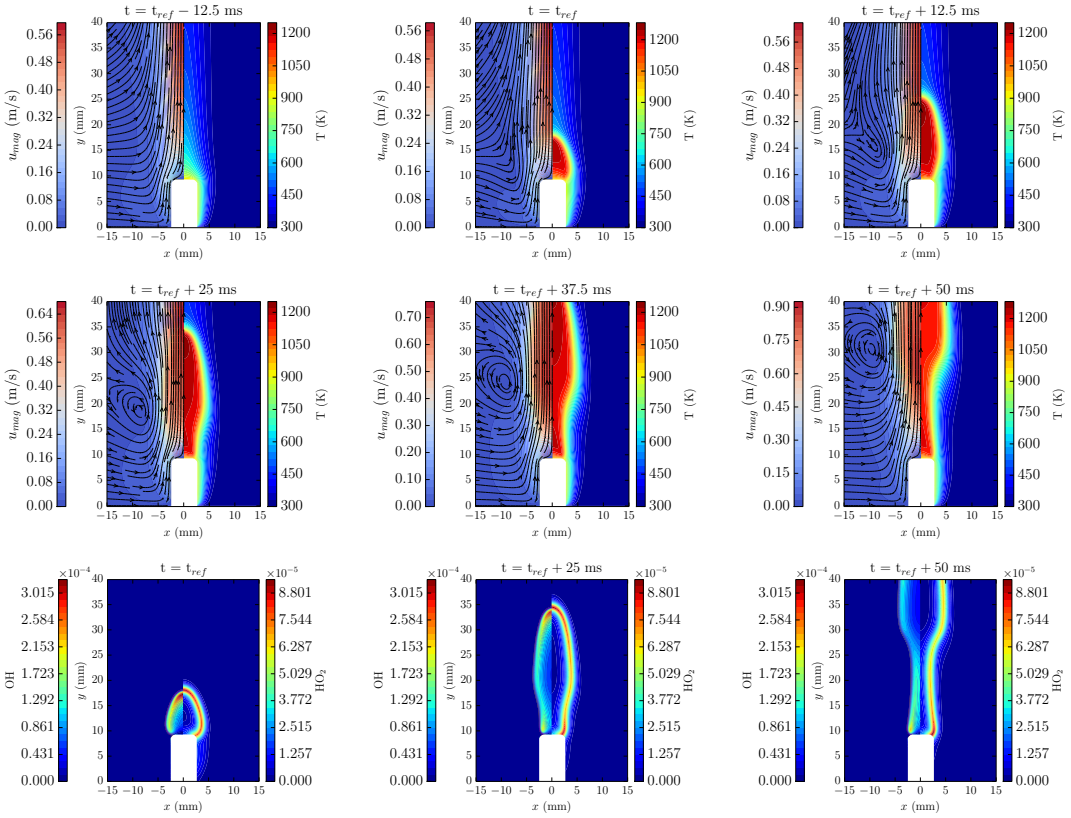

Figure 3: Temperature and velocity (magnitude) fields, streamlines and radical mass fraction fields during ignition and flame propagation for a 5% hydrogen in air mixture.

reaction develops at $t = t_{ref} + 40\,\mathrm{ms}$ at the outer top edge of the glow plug, $y \approx 10\,\mathrm{mm}$, $x \approx 2.5\,\mathrm{mm}$, and stabilizes. Later times are shown in the third row of Fig. 2. High temperature is observed in the plume above the glow plug suggesting chemical reaction taking place. Spatial temperature fluctuations within the plume close to the symmetry axis at times $t_{ref} + 1\,\mathrm{s} \leq t \leq t_{ref} + 3\,\mathrm{s}$ are likely due to measurement inaccuracies related to the inverse Abel transformation of the interferometry results. No further ignition events occurred until the experiment was terminated at $t = 60\,\mathrm{s}$, which differentiates this ignition phenomenon from cyclic (puffing) flames.

5 Numerical simulation results

For $X_{\mathrm{H_2}} = 5\%$ the simulation predicts an ignition threshold of 938 K, 7.1% lower than the value reported experimentally (1010 K). The presented simulation field-of-view is slightly larger than in the experiment to capture additional flow features.

Rows 1 and 2 in Fig. 3 show temperature and velocity (magnitude) fields, along with velocity vectors revealing the flow dynamics inside the combustion vessel. Row 3 presents corresponding OH and HO_2 mass fractions. Ignition occurs at the glow plug top signified by an increase in temperature and OH and HO_2 mass fractions. At $t = t_{ref}$, a flame can be seen, propagating upward within the thermal plume. The flame does not propagate radially outwards beyond the thermal plume due to the low hydrogen concentration, which is below the limit for horizontal flame propagation of $X_{\mathrm{H_2}} \approx 6\%$ at the present initial conditions P_o, T_o. The maximum in velocity remains inside the plume indicating weak expansion of the gas during the ignition/flame propagation event. However, it does induce an appreciable horizontal velocity that disturbs the streamlines as shown at $t = t_{ref}$ compared to $t = t_{ref} - 12.5\,\mathrm{ms}$. This field

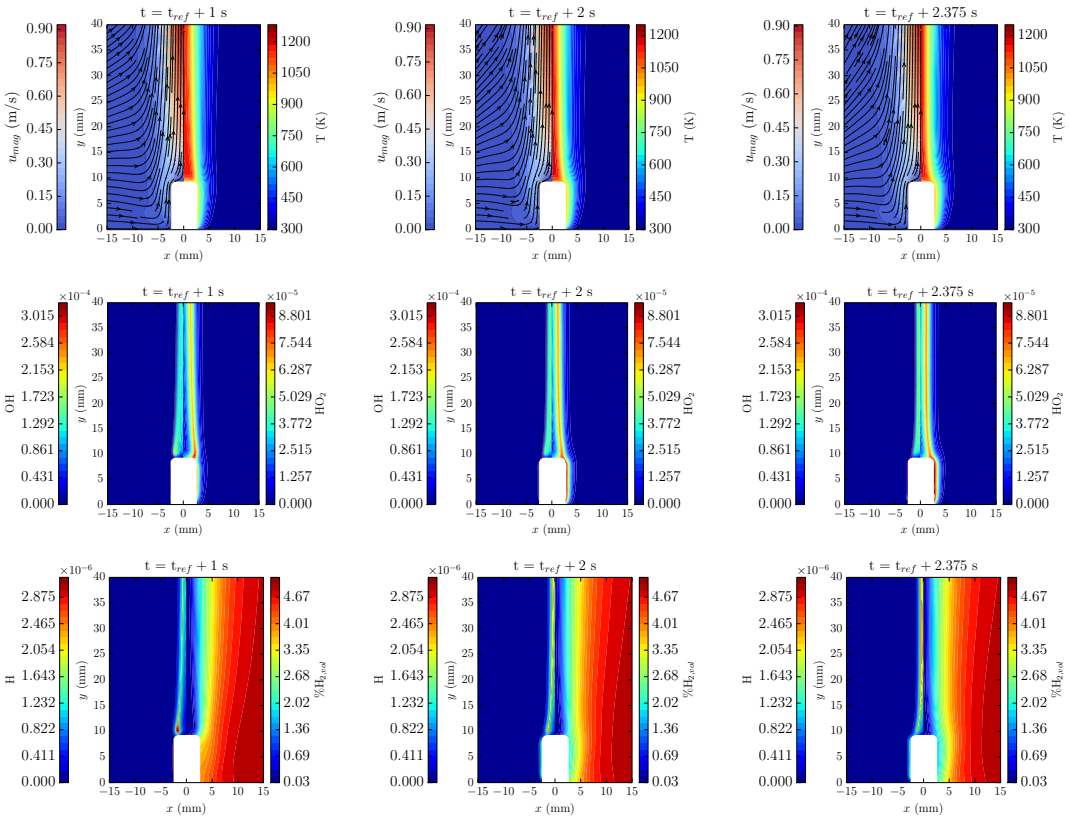

Figure 4: Temperature and velocity (magnitude) fields, streamlines, radical mass fraction and hydrogen concentration fields after ignition for a 5% hydrogen in air mixture.

compares very well with the experimental result at $t = t_{ref}$ in Fig. 2. The flame remains anchored at the outer top edge of the glow plug throughout the entire process. The temperature and velocity fields, and streamlines show the formation of a vortical structure at the edge of the flame, see for instance at $t = t_{ref}+25\,\mathrm{ms}$ at $y \approx 20\,\mathrm{mm}$ and $x \approx -10\,\mathrm{mm}$, which leads to a localized concave deformation of the flame. This is the result of the horizontal velocity induced by the ignition event, radial flame propagation, and the vertical buoyancy flow induced by the heating of the glow plug. This vortex gets advected upwards, and results in complete detachment of the top portion of the flame at later times (not shown). The early stages of the vortex-flame interaction can be observed at $t_{ref} + 25\,\mathrm{ms} \leq t \leq t_{ref} + 50\,\mathrm{ms}$ around $y = 25\,\mathrm{mm}$, Fig. 3. The evolution just described is consistent with the experimental observations in Fig. 2.

Figure 4 shows the flow field (row 1), OH and HO_2 mass fractions (row 2), and H mass fraction and hydrogen concentration (row 3), 1 s, 2 s and 2.375 s after ignition. The numerical integration was not carried out for the entire experiment duration of 60 s due to limitations in computational time. A vertical "tube" of combustion products is observed, fed by reactants from the sides of the glow plug. Production of OH decays from $t = t_{ref}+50\,\mathrm{ms}$ to $t = t_{ref}+1\,\mathrm{s}$, whereas HO_2 continues to be strong at the top edge and side of the hot surface. One second after ignition the sides of the glow plug are surrounded by mixture that is slightly below the lower flammability limit of hydrogen-air mixtures of 4%, see Fig. 4, row 3. At $t = t_{ref} + 2\,\mathrm{s}$ and $t = t_{ref} + 2.375\,\mathrm{s}$, the fields show a further decrease in hydrogen content with values ranging from 1–3% within the thermal boundary layer. There seems to be partial conversion of H_2 to HO_2 but not enough H atoms present to result in the production of OH through reaction H + HO_2 $\rightarrow$ OH + OH. In agreement with the experiment no further ignition events are observed in the simulation.

6 Conclusions

The dynamics of ignition from a hot surface near the flammability limits of premixed hydrogen-air were studied in a combined experimental and numerical approach. In addition to the known cyclic (puffing) combustion phenomenon, we observed singular ignition events (single puff) near the lean flammability limit. A flame kernel forms at the hot surface, and the buoyant flame travels upward within the thermal plume accompanied by a propagating vortical structure. The flame only expands weakly in the horizontal direction and anchors at the surface edges, feeding a hot plume with combustion products. Despite high surface temperatures, no further ignition events occur. A layer of non-flammable mixture develops around the hot surface and shields it from the fresh surrounding mixture. The described ignition phenomenon does not lead to a significant pressure increase in the closed combustion vessel.

Acknowledgements

This work was performed at the Explosion Dynamics Laboratory at the California Institute of Technology and was supported by The Boeing Company through a Strategic Research and Development Relationship Agreement CT-BA-GTA-1.

References

[1] P.A. Boettcher, S.K. Menon, B.L. Ventura, G. Blanquart, and J.E. Shepherd. Cyclic flame propagation in premixed combustion. *Journal of Fluid Mechanics*, 735:176–202, 2013.

[2] P.A. Boettcher. *Thermal ignition*. PhD thesis, California Institute of Technology, 2012.

[3] R. Mével, J. Melguizo-Gavilanes, L.R. Boeck, and J.E. Shepherd. Experimental and numerical study of the ignition of hydrogen-air mixtures by a localized stationary hot surface. *Article in preparation*, 2017.

[4] Q. Kemao. Windowed fourier transform for fringe pattern analysis. *Applied Optics*, 43(13):2695–2702, 2004.

[5] G. Pretzler. A new method for numerical Abel-inversion. *Zeitschrift für Naturforschung*, 46:639–641, 1991.

[6] W.C. Gardiner, Y. Hidaka, and T. Tanzawa. Refractivity of combustion gases. *Combustion and Flame*, 40:213–219, 1981.

[7] T. Poinsot and D. Veynante. *Theoretical and Numerical Combustion*. Edwards, 2005.

[8] J. Melguizo-Gavilanes, L.R. Boeck, R. Mével, and J.E. Shepherd. Hot surface ignition of stoichiometric hydrogen-air mixtures. *International Journal of Hydrogen Energy*, 2016.

[9] H.G. Weller, G. Tabor, H. Jasak, and C. Fureby. A tensorial approach to computational continuum mechanics using object-oriented techniques. *Computers in Physics*, 12(6):620–631, 1998.

[10] R. Mével, S. Javoy, F. Lafosse, N. Chaumeix, G. Dupré, and C.E. Paillard. Hydrogen-nitrous oxide delay time: shock tube experimental study and kinetic modelling. *Proceedings of The Combustion Institute*, 32:359–366, 2009.

[11] R. Mével, S. Javoy, and G. Dupré. A chemical kinetic study of the oxidation of silane by nitrous oxide, nitric oxide and oxygen. *Proceedings of The Combustion Institute*, 33:485–492, 2011.

View publication stats